

Metadata of the article that will be visualized in OnlineFirst

ArticleTitle	Biochemical and spectroscopic characterizations of the oligomeric antennas of the coral symbiotic <i>Symbiodiniaceae Fugacium kawagutii</i>	
Article Sub-Title		
Article Copy Right	The Author(s), under exclusive licence to Springer Nature B.V. (This will be the copyright line in the final PDF)	
Journal Name	Photosynthesis Research	
Corresponding Author	FamilyName	Niedzwiedzki
	Particle	
	Given Name	Dariusz M
	Suffix	
	Division	Center for Solar Energy and Energy Storage
	Organization	Washington University in St. Louis
	Address	St. Louis, MO, 63130, USA
	Division	Department of Energy Environmental and Chemical Engineering
	Organization	Washington University in St. Louis
	Address	St. Louis, MO, 63130, USA
	Phone	
	Fax	
	Email	niedzwiedzki@wustl.edu
	URL	
	ORCID	
Corresponding Author	FamilyName	Liu
	Particle	
	Given Name	Haijun
	Suffix	
	Division	Department of Biology
	Organization	Washington University in St. Louis
	Address	St. Louis, MO, 63130, USA
	Phone	
	Fax	
	Email	liuhaijun@wustl.edu
	URL	
	ORCID	http://orcid.org/0000-0003-0537-0302
Author	FamilyName	Magdaong
	Particle	
	Given Name	Nikki Cecil M
	Suffix	
	Division	Department of Chemistry
	Organization	Washington University in St. Louis
	Address	St. Louis, MO, 63130, USA
	Phone	
	Fax	
	Email	
	URL	
	ORCID	
Author	FamilyName	Su
	Particle	
	Given Name	Xinyang
	Suffix	
	Division	Department of Biology
	Organization	Washington University in St. Louis
	Address	St. Louis, MO, 63130, USA
	Phone	
	Fax	
	Email	
	URL	
	ORCID	

Schedule	Received	19 May 2022
	Revised	
	Accepted	16 Aug 2022
Abstract	<p>Light-harvesting antennas in photosynthesis capture light energy and transfer it to the reaction centers (RCs) where photochemistry takes place. The sustainable growth of the reef-building corals relies on a constant supply of the photosynthates produced by the endosymbiotic dinoflagellate, belonging to the family of <i>Symbiodiniaceae</i>. The antenna system in this group consists of the water-soluble peridinin-chlorophyll <i>a</i>-protein (PCP) and the intrinsic membrane chlorophyll <i>a</i>-chlorophyll <i>c</i>₂-peridinin protein complex (acpPC). In this report, a nonameric acpPC is reported in a dinoflagellate, <i>Fugasium kawagutii</i> (formerly <i>Symbiodinium kawagutii</i> sp. CS-156). We found that extensive biochemical purification altered the oligomerization states of the initially isolated nonameric acpPC. The excitation energy transfer pathways in the acpPC nonamer and its variants were studied using time-resolved fluorescence and time-resolved absorption spectroscopic techniques at 77 K. Compared to the well-characterized trimeric acpPC, the nonameric acpPC contains an 11 nm red-shifted terminal energy emitter and the substantially altered excited state lifetimes of Chl <i>a</i>. The observed energetic overlaps of the fluorescence terminal energy emitters with the RCs' absorption are hypothesized to enable efficient downhill excitation energy transfer. Additionally, the shortened Chl <i>a</i> fluorescence decay lifetimes in the oligomeric acpPC indicate a protective self-relaxation strategy. We propose that the highly oligomerized acpPC nonamer represents an intact functional unit in the <i>Symbiodiniaceae</i> thylakoid membrane. They perform efficient excitation energy transfer (to RCs), and are under manageable regulations in favor of photoprotection.</p>	
Keywords (separated by '-')	LHC - Symbiodiniaceae - acpPC - Oligomer - Transient absorption - Time-resolved fluorescence	
Footnote Information	The online version contains supplementary material available at https://doi.org/10.1007/s11120-022-00951-6 .	



2 Biochemical and spectroscopic characterizations of the oligomeric 3 antennas of the coral symbiotic *Symbiodiniaceae Fugacium kawagutii*

4 Dariusz M. Niedzwiedzki^{1,2} · Nikki Cecil M. Magdaong³ · Xinyang Su⁴ · Haijun Liu⁴

5 Received: 19 May 2022 / Accepted: 16 August 2022
6 © The Author(s), under exclusive licence to Springer Nature B.V. 2022

7 Abstract

8 Light-harvesting antennas in photosynthesis capture light energy and transfer it to the reaction centers (RCs) where photo-
9 chemistry takes place. The sustainable growth of the reef-building corals relies on a constant supply of the photosynthates
10 produced by the endosymbiotic dinoflagellate, belonging to the family of *Symbiodiniaceae*. The antenna system in this group
11 consists of the water-soluble peridinin-chlorophyll *a*-protein (PCP) and the intrinsic membrane chlorophyll *a*-chlorophyll
12 *c*₂-peridinin protein complex (acpPC). In this report, a nonameric acpPC is reported in a dinoflagellate, *Fugacium kawagutii*
13 (formerly *Symbiodinium kawagutii* sp. CS-156). We found that extensive biochemical purification altered the oligomeriza-
14 tion states of the initially isolated nonameric acpPC. The excitation energy transfer pathways in the acpPC nonamer and
15 its variants were studied using time-resolved fluorescence and time-resolved absorption spectroscopic techniques at 77 K.
16 Compared to the well-characterized trimeric acpPC, the nonameric acpPC contains an 11 nm red-shifted terminal energy
17 emitter and the substantially altered excited state lifetimes of Chl *a*. The observed energetic overlaps of the fluorescence
18 terminal energy emitters with the RCs' absorption are hypothesized to enable efficient downhill excitation energy transfer.
19 Additionally, the shortened Chl *a* fluorescence decay lifetimes in the oligomeric acpPC indicate a protective self-relaxation
20 strategy. We propose that the highly oligomerized acpPC nonamer represents an intact functional unit in the *Symbiodiniaceae*
21 thylakoid membrane. They perform efficient excitation energy transfer (to RCs), and are under manageable regulations in
22 favor of photoprotection.

23 **Keywords** LHC · Symbiodiniaceae · acpPC · Oligomer · Transient absorption · Time-resolved fluorescence

24 Introduction

25 Photosynthesis is a process in which light energy is har-
26 vested and converted to chemical energy to sustain life and
27 evolution. Two of the early events in photosynthesis, i.e.,

light capture and photochemical conversion, are accom- 28
plished by two types of pigmented-protein complexes 29
(PPCs): light-harvesting antenna complexes (LHCs), which 30
are responsible for photon absorption and transfer of the 31
excitation energy, and the reaction centers (RCs), where 32
primary photochemistry occurs. Compared to the relatively 33
conserved RCs, a variety of light-harvesting complexes has 34
evolved to match the photosynthetic organisms' eco-physi- 35
ological niche (Blankenship 2002). 36

Dinoflagellates in the family of *Symbiodiniaceae* are impor- 37
tant photosynthetic symbionts in cnidarians (such as corals) 38
and other coral reef organisms. They have evolved two unique 39
types of LHCs: the peridinin-chlorophyll *a*-protein (PCP) 40
and the chlorophyll *a*-chlorophyll *c*₂-peridinin-protein com- 41
plex (acpPC) (Hiller et al. 1993, 1995; Hofmann et al. 1996; 42
Sharples et al. 1996; Schulte et al. 2009a, b; Schulte et al. 43
2010). PCP is a water-soluble complex residing in the thyla- 44
koid lumen. PCP contains peridinin, a structurally complex 45
carotenoid, as a primary photosynthetic pigment, which, upon 46

A1 ✉ Dariusz M. Niedzwiedzki
A2 niedzwiedzki@wustl.edu

A3 ✉ Haijun Liu
A4 liuhaijun@wustl.edu

A5 ¹ Center for Solar Energy and Energy Storage, Washington
A6 University in St. Louis, St. Louis, MO 63130, USA

A7 ² Department of Energy Environmental and Chemical
A8 Engineering, Washington University in St. Louis, St. Louis,
A9 MO 63130, USA

A10 ³ Department of Chemistry, Washington University
A11 in St. Louis, St. Louis, MO 63130, USA

A12 ⁴ Department of Biology, Washington University in St. Louis,
A13 St. Louis, MO 63130, USA

excitation, transfers the energy to chlorophyll *a* (Chl *a*). Structural and spectroscopic studies of PCP have greatly advanced our understanding of this antenna complex (Hofmann et al. 1996; Zigmantas et al. 2002; Ilagan et al. 2006; Schulte et al. 2009a, b; van Stokkum et al. 2009; Niedzwiedzki et al. 2013). However, it remains unclear how the membrane extrinsic PCP interacts with the thylakoid membrane and what the route is of the excitation energy migration from PCP to the RCs (Reynolds et al. 2008; Kanazawa et al. 2014).

acpPC in *Symbiodiniaceae* is an intrinsic membrane protein complex, belonging to the LHC protein superfamily (Durnford et al. 1999). In comparison to PCP, acpPC has much higher abundance in the algal cells (Iglesiasprieto et al. 1991). It was revealed that acpPC consists of a group of polypeptides with molecular weight (MW) of 18–20 kDa. Spectroscopic studies indicated that both peridinin and Chl *c*₂ pigments transfer excitations to Chl *a*. It was postulated that the excitation energy transfer pathways involve the peridinin S₂ electronic excited state and S₁/ICT (intramolecular charge-transfer) states. The inter-pigment energy transfer yields are high, close to unity. The role of another carotenoid, diadinoxanthin, found in the antenna complex, is still unclear (Polivka et al. 2006; Di Valentin et al. 2010; Slouf et al. 2013; Niedzwiedzki et al. 2014). As aforementioned, acpPC has been the subject of research using various molecular spectroscopic techniques, the investigations on the possible oligomerization states and their relationships to the pigments' energetic landscape in acpPC, however, are scarce. Our previous study provided the first evidence that the functional state of acpPC is a trimer (Jiang et al. 2014), in analogy to other LHC superfamily proteins from photosynthetic eukaryotes (Liu et al. 2004; Buchel 2015). It remains unclear, however, if there exist any higher order oligomerization states of acpPC, if yes, how they are functionally and structurally different than the well-characterized trimeric acpPC.

In this study, we report two acpPC samples with apparently different higher order oligomeric organizations and their subsequent spectroscopic characterizations. This study also showcases that the oligomerization states of the acpPC complex can be altered, and the pigment content decreases upon further biochemical processing. Through the applications of time-resolved absorption and fluorescence emission spectroscopies performed at 77 K, we have studied whether alterations of the oligomerization states of acpPC affect excitation energy transfer.

Materials and methods

Algal culture and isolation of acpPC protein

Fugacium kawagutii (formerly *Symbiodinium kawagutii* sp. CS-156 cells) cells were cultured in *f/2* media under diurnal

cycle (14 h:10 h of light: dark) at 25 °C. Briefly, Guillard's (*f/2*) marine water enrichment solution (Sigma-Aldrich, St. Louis, MO) was diluted in filtered, sterile seawater to achieve the reconstituted growth media. Illumination was provided by an array of white colored fluorescent lamps at an intensity of 50 μmol photons·m⁻²·s⁻¹. The culture in late exponential growth phase (after 3–4 weeks) was harvested by centrifugation at 6000 rpm using Sorvall SLC-6000 centrifuge bottles at 4 °C. Cell pellets were resuspended in MMB buffer containing 20 mM 2-morpholinoethanesulfonic acid (MES) at pH 6.3, 5 mM MgCl₂, and 1 M betaine, and saved in –80 °C until ready to use. Subsequently, cells were disrupted by passing twice through French press, with the French press cell prechilled at 4 °C, at 8 × 10⁷ Pa, and a protease inhibitor cocktail (A32965, Pierce, Thermo-Fisher Scientific, Waltham, MA) and deoxyribonuclease (DN25-1G, Sigma-Aldrich, St. Louis, MO) added and completely dissolved. The cell lysate was centrifuged at 2000×*g* for 5 min to dispose the unbroken cells, and the supernatant was then centrifuged at 100,000×*g* for 30 min to collect the thylakoid membrane particles. The pellet was then resuspended and homogenized with a paintbrush in MBNC buffer containing 20 mM MES at pH 6.3, 1 M betaine, 10 mM NaCl, and 5 mM CaCl₂ to a Chl *a* concentration of 1.0 mg/mL. The membranes were then solubilized to a 1% (v/v) *n*-dodecyl-β-D-maltopyranoside (β-DDM) final concentration, for 15 min in the dark with gentle stirring. In the next step, the sample was centrifuged at 30,000×*g* for 20 min to remove the insoluble debris, and the supernatant was then loaded onto the sucrose density step gradient (SDG) ultracentrifugation tubes containing 0.1, 0.4, 0.7, 1.0, 1.3 M sucrose in 25 mM HEPES buffer (pH 7.0, 1 M betaine, 0.04% β-DDM). After centrifugation at 160,000×*g* for 18 h, the bands containing the acpPC fraction (SDG-acpPC) were collected for purity and spectroscopic analysis. Collected SDG-acpPC sample was further purified using ion exchange chromatography (IEC) (HiTrap Q HP column, Sigma-Aldrich, St. Louis, MO) with BioLogic DuoFlow Medium-Pressure Chromatography Systems (Bio-Rad, Hercules, CA). Linear gradient of NaCl from 15 to 200 mM in MBNC buffer was used to elute the sample. Protein samples were desalted and concentrated using 100 kDa MWCO Amicon Ultra-15 centrifugal filters (Millipore-Sigma, St. Louis, MO). The flow-through was further desalted and concentrated using Ultra-15 centrifugal filters (30 kDa MWCO, Millipore-Sigma, St. Louis, MO) and was named SDG-IEC^{FT}. Determination of acpPC protein oligomerization states in SDG, SDG-IEC and SDG-IEC^{FT} preparations was performed using blue native gel (Schagger and von Jagow 1991).

145 **Pigment analysis of acpPC**

146 The pigment composition of the initial complex (SDG-
147 acpPC) was determined using high performance liquid
148 chromatography (HPLC, Agilent, Santa Clara, CA). Pig-
149 ments were extracted from an aliquot (~25 μL) of the band
150 collected after SDG ultracentrifugation (Fig. 1a) by mix-
151 ing the sample with methanol. The mixture was vortexed
152 for a few seconds, followed by centrifugation at $9400\times g$
153 for 1 min. The supernatant was carefully collected and
154 dried under N_2 air on ice and dim light. The dried extract
155 was then resuspended with 100 μL of acetonitrile (70:30
156 v/v), filtered and injected into an Agilent HPLC Series
157 1100 equipped with a Zorbax Eclipse XDB C18 column.
158 The flow rate of the mobile phase was set to 1 mL/min,
159 starting with an isocratic flow of 99% Solvent A (87:10:3
160 v/v/v acetonitrile/methanol/water) and 1% Solvent B
161 (100% ethyl acetate) for 15 min, followed by a linear gra-
162 dient to 40 min to a solvent composition of 60% Solvent
163 A and 40% Solvent B. Data were collected and analyzed
164 using Agilent Openlab CDS Chemstation software.

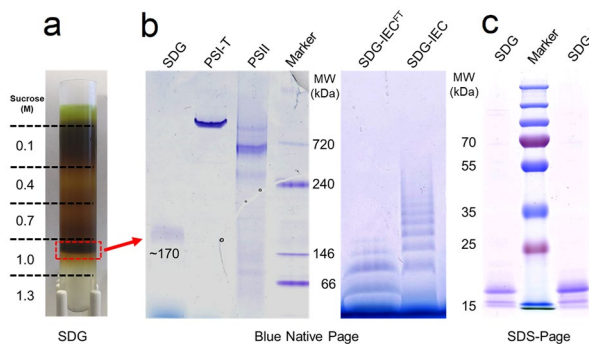


Fig. 1 Separation and biochemical characterizations of oligomeric form of acpPC antenna from *Fugacium kawagutii*. **a** SDG separation of solubilized thylakoid membrane. Sucrose concentration (M) of each step is labelled. Red square (dashed line) indicated sample is subjected for analysis. **b** Blue native page analysis of the most intense band loaded directly after centrifugation (SDG, left panel) or after additional purification with ion exchange chromatography and subsequent concentration using 100 kDa (MWCO) filtration (SDG-IEC, right panel). The flowthrough (FT) from 100 kDa ultrafiltration was further concentrated using 30 kDa (MWCO) filtration, the retentate is denoted as SDG-IEC^{FT}, but not subjected for further analysis. SDG reveals single band with MW of ~170 kDa. Further processing of the band through IEC/ultrafiltration altered the original oligomeric state resulting several oligomeric forms as indicated by ladder-like band pattern. **(c)** SDS-PAGE analysis of SDG- and SDG-IEC-acpPC. *PSII*—photosystem II from a cyanobacterium, *Synechocystis* sp. PCC 6803, *PSI-T*—photosystem I trimer from *Synechocystis* sp. PCC 6803, *MW*—molecular weight, *SDG*—sucrose density gradient, *SDS*—sodium dodecyl sulfate

165 **Femtosecond time-resolved transient absorption spectroscopy** 166

167 Time-resolved pump-probe absorption (TA) experiments were
168 carried out using Helios, a femtosecond transient absorption
169 spectrometer (Ultrafast Systems, Sarasota, FL) coupled to
170 a femtosecond laser system previously described in detail
171 (Niedzwiadzki et al. 2011). The acpPC sample was excited at
172 540 nm, preferentially corresponding to the peridinin absorp-
173 tion. The energy of the pump beam was set to 200 nJ in a spot
174 size of 1 mm diameter corresponding to a laser flux of $\sim 10^{14}$
175 photons cm^{-2} .

176 **Time-resolved fluorescence spectroscopy**

177 Time-resolved fluorescence (TRF) experiments were carried
178 out using a Hamamatsu universal streak camera consisting of
179 a cooled N51716-04 streak tube, C5680 blanking unit, digital
180 CCD camera (Orca2), slow speed M5677 unit, C10647 and
181 C1097-05 delay generators and an A6365-01 spectrograph
182 from Bruker. Excitation pulses at 540 nm were produced by an
183 ultrafast optical parametric oscillator (OPO) Inspire100 (Spec-
184 tra-Physics, Milpitas, CA) pumped with a Mai-Tai ultrafast
185 Ti:Sapphire laser (Spectra-Physics, Milpitas, CA), generat-
186 ing ~90 fs laser pulses at 820 nm with a frequency of 80 MHz.
187 After OPO, the frequency of excitation beam was lowered
188 to 4 MHz (250 ns between subsequent excitations) by 3980
189 Pulse Selector equipped with 3986 controller (Spectra-Physics,
190 Milpitas, CA). Excitation beam with power of ~10 mW was
191 focused on the sample in a circular spot of 2 mm diameter
192 which corresponds to $\sim 10^{10}$ photons $\cdot \text{cm}^{-2}$.

193 **Spectroscopic data processing and global analysis**

194 Surface Xplorer 4 (Ultrafast Systems, Sarasota, FL) was
195 used to correct the dispersion present in the TA. Global fit-
196 ting of TRF and TA datasets was performed using Carpet-
197 View (Light Conversion, Vilnius, Lithuania) with so-called
198 target modeling that uses anticipated kinetic models (van
199 Stokkum et al. 2004). The fitting included convolution of the
200 data with Gaussian-like instrument response function hav-
201 ing a full width at the half maximum of ~200 fs for Helios
202 (TA) and ~0.35 ns for streak camera setup (TRF). All plots
203 were done in Origin 2021b (Origin Lab Corp., Northampton,
204 MA).

205 **Results**206 **Oligomeric states of acpPC**

207 The isolated acpPC complex from *Fugacium kawagutii* is
208 evidently different than the one previously reported (Polivka

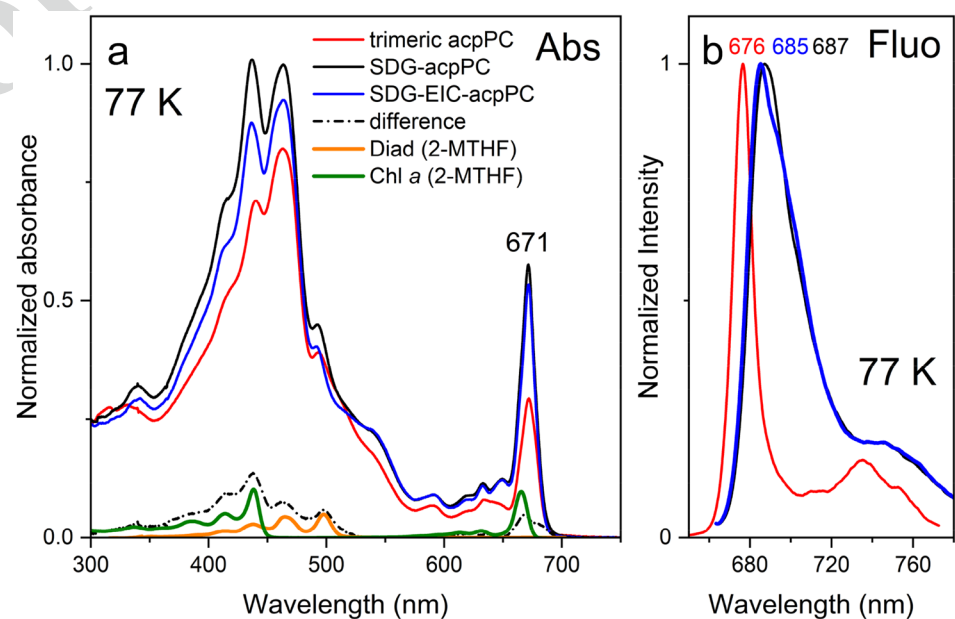
209 et al. 2006, Slouf et al. 2013; Jiang et al. 2014). For the
 210 current preparation, the thylakoid membranes were initially
 211 solubilized by β -DDM in the presence of 1 M betaine and
 212 then subjected to SDG ultracentrifugation, resulting in three
 213 major bands (Fig. 1a). We proceeded with the most abundant
 214 fraction (marked with a red rectangle) for further analysis.
 215 The functional acpPC has been previously identified as a
 216 trimer with molecular weight (MW) of 66.5 kDa and the
 217 apo-peptide subunit of 18.3 kDa (Jiang et al. 2014). Our cur-
 218 rent preparation, however, represents a novel oligomeriza-
 219 tion state of acpPC, with MW of 170–180 kDa as estimated
 220 using Blue Native gel (BN-gel) analysis (Fig. 1b, SDG). The
 221 BN-gel is usually employed to estimate MW and the oli-
 222 gomerization states of the native protein complexes provided
 223 the MW of the base subunit is known (Schagger and von
 224 Jagow 1991). Note that there is no indication of any pres-
 225 ence of photosystems (PSI, PSII) associated with this band.
 226 The SDS-PAGE analysis of the acpPC complex (Fig. 1c)
 227 indicates the MW of the major band as 18 kDa with some
 228 microheterogeneity, which seems consistent with our previ-
 229 ous report on the same species (Jiang et al. 2014). There-
 230 fore, the SDG-acpPC sample was assigned to be a nonamer,
 231 most likely a trimer of the previously characterized trimeric
 232 acpPC (acpPC^{3×3} vs acpPC³) (Jiang et al. 2014). Inter-
 233 estingly, BN-gel analysis on the sample SDG-EIC-acpPC,
 234 Fig. 1b right panel) reveals that the nonamer may have bro-
 235 ken down and then reaggregated (reassembled), forming a
 236 ladder-like appearance of multiple bands with MW consist-
 237 ing of subunit multiples (Fig. 1a, b, SDG vs. SDG-EIC vs.
 238 SDG-IEC^{FT}). Protein subunit analysis (SDS-PAGE) on the
 239 SDG-acpPC and SDG-EIC-acpPC did not detect any composi-
 240 tional difference. Apparently, further purification of the
 241 SDG-acpPC using IEC and subsequent ultrafiltration altered

the nonameric state of the SDG-acpPC and triggered the
 formation of a mixture of numerous oligomers (Fig. 1b).
 The 100-kDa filter (MWCO) flowthrough of the SDG-IEC
 sample was collected and further concentrated using 30 kDa
 filter. The oligomerization states of the sample were ana-
 lyzed (Fig. 1b, SDG-IEC^{FT}), but was not subjected for fur-
 ther spectroscopic analysis.

Steady-state absorption and fluorescence emission

To address whether the disassembly and then reassembly
 (reaggregation) of acpPC (Fig. 1b, right panel) is associ-
 ated with any loss of the pigments, the pigment compositions
 of SDG-acpPC and SDG-IEC-acpPC were compared. First-
 ly, the pigment content was determined using HPLC equip-
 ped with photodiode array (Fig. S1). This analysis showed
 that the pigment contents remain unchanged compared to
 those of the trimeric acpPC. Note, pigments² identifica-
 tion was done according to their elution times and absorp-
 tion spectra, which seems, respectively, consistent with our
 previous studies (Niedzwiedzki et al. 2014). Subsequently,
 to find out if any pigments are lost during in SDG-acpPC
 and SDG-IEC-acpPC, a basic spectral analysis of absorp-
 tion spectra of both preparations was performed. This sub-
 ject was better evaluated by taking absorption spectra at
 77 K, since cryogenic temperature enhances spectral dif-
 ferences. The spectra are shown in Fig. 2a. The black
 spectrum corresponds to the oligomeric (nonamer) acpPC
 complex, and the blue spectrum corresponds to the same
 batch sample which was additionally purified using IEC
 and then concentrated (SDG-IEC-acpPC). The spectral
 normalization at 590 nm was under the assumption that
 sample absorbance at this wavelength should be least af-
 fected by further acpPC purification. The

Fig. 2 a 77 K steady-state absorption (Abs) and fluorescence emission (Fluo) spectra of trimeric and oligomeric forms (SDG-acpPC, SDG-EIC-acpPC) of the acpPC complex from *Fragarium kowagutii*. The absorption spectra are normalized at 590 nm upon assumption that Chl *c*₂ content will be minimally affected by post-SDG purification/processing. Difference spectrum (red dash-dot, SDG-minus-SDG-EIC) shows that further sample processing removes some fraction of Chl *a* and diadinoxanthin (Diad). The difference spectrum is very similar to the sum of the reference spectra of both pigments taken in 2-MTHF at 77 K (spectrally shifted to match peak positions)



band around 590 nm is mostly associated with absorption of Chl c_2 and therefore, we tentatively assumed that stoichiometry of this pigment does not change between preparations. Such expectation originates from the fact that pigment arrangements in the structure of the monomeric acpPC of this species could be similar to the one recently revealed in the FCP complex from the diatom *Phaeodactylum tricornutum* (Wang et al. 2019). The FCP complex shows significantly high similarity in its pigment content to the acpPC, however, instead of peridinin it binds the carotenoid fucoxanthin. The structure of FCP monomer shows two molecules of Chl c_2 centrally bound in the complex, surrounded by a layer of multiple Chl a and fucoxanthin and one peripherally bound diadinoxanthin. If such Chl c_2 binding chemistry is conserved and maintained in acpPC, we might expect that the disassembly occurring during IEC processing should have minimal stripping effects on the central Chl c_2 . The Chl a and diadinoxanthin molecules located on the peripheral regions of acpPC and thus on the interfaces between acpPC subunits of an oligomeric acpPC, however, tend to be easily lost. Indeed, the difference spectrum (Fig. 2a, black dash-dot) could be very well mimicked by a sum of the individual 77 K absorption spectra of Chl a (green) and diadinoxanthin (orange) recorded in 2-MTHF, adequately shifted to match their peak positions. It confirms that upon further purification and subsequent concentration of oligomeric acpPC, some fractions of peripherally bound Chl a and diadinoxanthin were permanently lost from the protein structure. For reference, the 77 K absorption spectrum of a previously studied acpPC trimer was also added for comparison (Jiang et al. 2014; Niedzwiedzki et al. 2014). This spectrum was intuitively normalized with that of the SDG-IEC-acpPC at 510 nm, upon an assumption that absorbance of the latter should not overpass the former at any wavelength. The spectral shape clearly reveals that the trimeric acpPC lacks a substantial pool of Chls a and carotenoids from its structure compared to the nonameric acpPC (Fig. 2b, green line and orange line). Consequently, even at this point, we might hypothesize that migration of the excitation energy within the nonamer and previously purified acpPC trimer could be substantially altered.

Although the absorption spectra of all the acpPC complexes show the Q_y band of Chl a at 671 nm, major differences between the trimeric acpPC and SDG- and SDG-IEC-acpPC are clearly observed in the fluorescence emission spectra (Fig. 2b). Note, these spectra, normalized for better comparability, were obtained by time-integration of time-resolved fluorescence profiles, which are provided in the next section. The spectra show that partial loss of Chl a and diadinoxanthin in SDG-IEF-acpPC does not cause substantial alterations of the emission band with respect to SDG-acpPC, probably because major population of Chls a associated with emission still remains intact. Although some

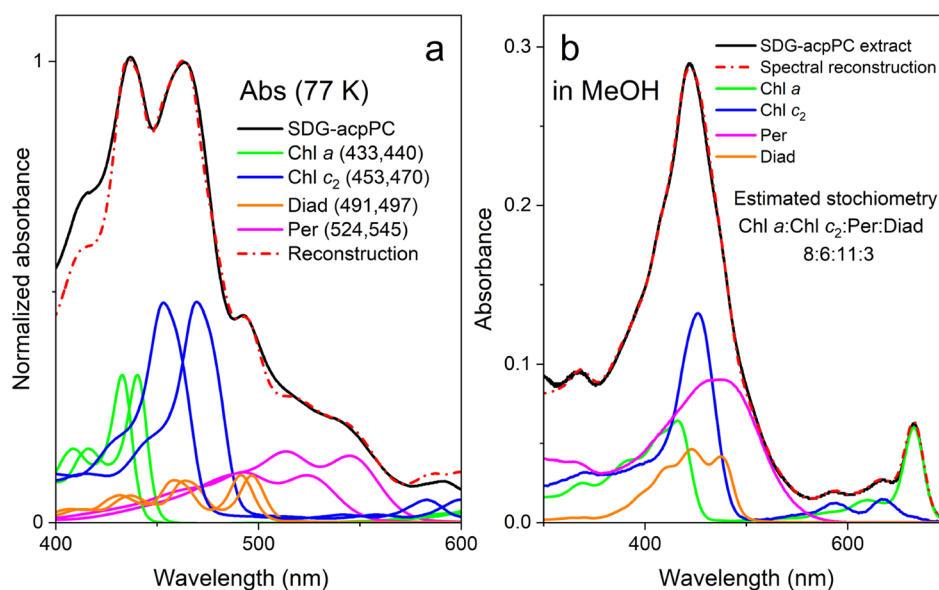
peak shifting/narrowing in the SDG-IEC-acpPC profile is noticeable (Fig. 2b). The differences between these two acpPC complexes and the trimeric acpPC are substantial. The fluorescence emission spectrum of the trimeric acpPC is narrower and its maximum is shifted to shorter wavelength (from 685 to 688 nm–676 nm).

Spectral reconstruction of absorption spectrum and determination of pigment stoichiometry

The absorption difference profile (Fig. 2a) can be adequately mimicked by the sum of the individual 77 K absorption spectra of Chl a and diadinoxanthin. This makes the spectral reconstruction of the main absorption band (400–600 nm) of the SDG-acpPC absorption spectrum feasible—those will be approximated positions of the absorption spectra of two classes of pigments bound to the complex. The attempt is demonstrated in Fig. 3a. The absorption spectra of each individual pigments recorded at 77 K in 2-MTHF were used, with their spectra shifted to optimal positions and adjusted in amplitudes for the best agreement. Note that in all cases, two different spectral forms were necessary for proper spectral modelling. The reconstructed vs. the experimental spectra do match well except in the 400–430 nm spectral range, suggesting that the amplitudes of the B bands in the Chl a absorption spectrum can be elevated if the pigment is buried into the complex. In addition, a small energetic spacing between the absorption spectra of diadinoxanthin may suggest that in acpPC, the carotenoid is represented by just one spectral form with broader vibronic bands, possibly due to the protein-driven geometric distortion of the conjugated part of the molecule, which, however, is not the case in the 2-MTHF glass.

The pigment stoichiometry in the SDG-acpPC was calculated based on the spectral reconstruction of the methanol extracts of the complex using the absorption spectra of each individual pigments recorded in methanol (Fig. 3b). The detailed procedure is provided in the Supplementary Information and in Fig S2. Our estimate gives Chl a :Chl c_2 :Per:Diad pigment stoichiometry of 8:6:11:3. It is informative to put it in the context of the pigment contents of the light-harvesting complexes (monomers) for which the crystal structures are known. Therefore, for FCP from diatom Chl a :Chl c_2 :Cars is 7:2:7 and for major LHCII from plants, Chl a :Chl b :Cars is 8:6:4 (Cars – collective carotenoids) (Liu et al. 2004; Wang et al. 2019). If the theme of 7–8 Chl a per complex monomer is consistent across the whole protein superfamily, we might hypothesize that the fully intact acpPC will bind 8 Chl a , 6 Chl c_2 , 11 Per and 3 Diad. On the other hand, considering that the overall number of carotenoids bound to antenna ranges from 4 to 7, the estimate provided above should be divided by factor of 2 to give a better agreement. Considering the difference in absorption

Fig. 3 Spectral reconstruction of the absorption spectra of SDG-acpPC and its solvent extract. **a** Spectral reconstruction of 77 K absorption spectrum of the SDG-acpPC with the absorption spectra of each individual pigment taken at 77 K in 2-MTHF and adequately shifted. For Chls, position of the Soret band and for carotenoids, position of the (0–0) vibronic band is provided. **b** Spectral reconstruction of absorption spectrum of methanol extract of SDG-acpPC with absorption spectra of individual pigments taken in methanol. This analysis provides the estimated pigment stoichiometry in the complex. For more details on the procedure refer to SI



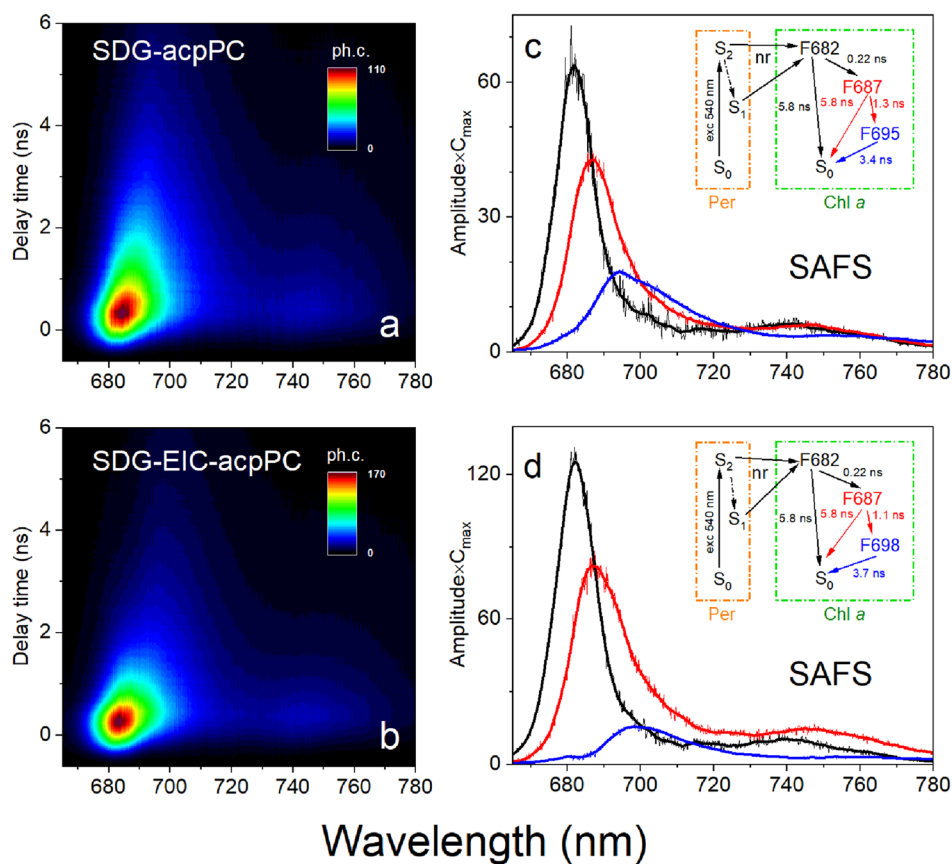
377 spectra of SDG- and SDG-IEC-acpPC complexes (Fig. 2a)
 378 and spectrum reconstruction of SDG-acpPC (Fig. 3a), it
 379 seems that further purification and processing of the com-
 380 plex causes 15–20% losses of Chl *a* and diadinoxanthin.

381 Time-resolved fluorescence imaging

382 The temporal characteristics of the fluorescence emission
 383 decay of Chl *a* in both SDG-acpPC and SDG-IEC-acpPC
 384 were investigated at 77 K. Previous 77 K time-resolved
 385 fluorescence analysis on the trimeric acpPC from the same
 386 organism demonstrated that, upon excitation of the carotenoid
 387 band, the excitation energy is promptly transferred
 388 to Chls and subsequently emitted as Chl *a* fluorescence. It
 389 is characterized by a single exponential component decay
 390 with a lifetime of 5.8 ns. No other kinetic components were
 391 revealed in the fluorescence decay profile (Niedzwiedzki
 392 et al. 2014). However, a very different scenario was observed
 393 in both SDG- and SDG-IEC-acpPC. Figure 4 presents the
 394 time-resolved fluorescence (TRF) imaging and subsequent
 395 spectro-temporal global analysis. The TRF images were
 396 recorded using very low excitation intensity at 540 nm,
 397 the spectral range that mostly coincides with the absorp-
 398 tion band of acpPC-bound peridinin (Polivka et al. 2006,
 399 Niedzwiedzki et al. 2014). It is known that upon direct
 400 excitation of peridinin in acpPC, the excitation is promptly
 401 and efficiently transferred to Chl *a*. Therefore, this selec-
 402 tion of excitation wavelength warrants that the entire Chl *a*
 403 fluorescence emission is associated with the protein-bound
 404 Chls *a*. The TRF decay images of the SDG-acpPC and SDG-
 405 IEC-acpPC (Fig. 4a, b) clearly reveal more complex fea-
 406 tures than those previously reported for the trimeric acpPC,
 407 but subtle differences also exist between two preparations

(SDG-acpPC and SDG-IEC-acpPC). Detailed information
 on the fluorescence emission dynamics can be achieved by
 performing global analysis of the TRF datasets (van Stok-
 kum et al. 2004). The outcomes of our fitting are provided
 in Fig. 4c, d. The data modelling was done according to the
 kinetic schemes provided in the figure insets. Hypothetically,
 the model should account for the fact that upon excitation
 at 540 nm (peridinin), excitation energy is transferred to
 Chl *a* collectively from the carotenoid singlet excited S_2
 and S_1 states. This process corresponds to the rise of Chl *a*
 fluorescence emission. However, as such process occurs in
 an ultrafast time regime (a few picoseconds) (Polivka et al.
 2006, Niedzwiedzki et al. 2014), the spectra cannot be tem-
 porally resolved due to the TRF technical setup limitations.
 Therefore, an applied fitting model to the experimental data
 must assume that the excitation directly populates/excites
 the first spectro-temporal fluorescence component detect-
 able in the data, which is already associated with Chl *a*.
 Overall, three spectro-temporal components were required
 to successfully model the TRF decay images in both cases.
 Because the data modelling was based on anticipated or so-
 called target model, the results were called species associ-
 ated fluorescence spectra (SAFS) and were denoted as F682,
 F687 and F695/698, based on approximate positions of their
 maxima expressed in nanometers. The first two SAFS also
 have competing intrinsic decays to the ground state fixed at
 5.8 ns, which corresponds to the intrinsic decay of excited
 monomeric Chl *a* in the trimeric acpPC (Niedzwiedzki et al.
 2014; Vinklerek et al. 2018). It could be interpreted that it is
 as if the oligomer falls apart into trimers, such that the vari-
 ous spectral species of Chl *a* will be reduced to one with a
 fluorescence lifetime of 5.8 ns (at 77 K).

Fig. 4 77 K time-resolved fluorescence (TRF) decay imaging of oligomeric acpPC after SDG and SDG-IEC, respectively. The samples were excited at 540 nm (Per—peridinin). **a, b** 2D pseudo-color TRF profiles in which colors represent emission intensities (photon counts, ph. c.). **c, d** Global analysis of fluorescence emission decay profiles. Refer to the main text for more details. The profiles were smoothed for better clarity. **SAFS**—species associated fluorescence spectra (smoothed for clarity), *nr*—not resolved, *F682–F698*—various Chl *a* fluorescence species



440 The SAFS were also corrected for their time dependent
 441 concentration in the TRF profile by multiplying the ampli-
 442 tude profiles by the maximum of time dependent concentra-
 443 tion, $C_{max}(t)$ (van Stokkum et al. 2004). This product more
 444 intuitively highlights the possible relative contributions of
 445 the components in the TRF data. The fitting demonstrates
 446 that there are three distinct Chl *a* spectral forms (Fig. 4c,
 447 d). Once the excitation enters the Chl *a* network, it is very
 448 quickly transferred to the more red-emissive pigments and
 449 ultimately trapped in the Chl *a* pool with fluorescence
 450 emission maximum at ~ 700 nm, which finally decays to the
 451 ground state. The dynamics of this process is very similar
 452 in both oligomeric forms of acpPC (SDG and SDG-IEC)
 453 though it is evident that the SDG sample has noticeably
 454 larger contributions of the energetically lowest (most red-
 455 shifted) fluorescence component. It strongly suggests that
 456 the further purification step performed after SDG alters the
 457 energetic landscape of the protein-bound Chls or it might
 458 be correlated with the observed $\sim 10\%$ loss of Chl *a* during
 459 post-SDG purification. Since SDG-IEC-acpPC is an ensemble
 460 with a large range of oligomerization extent (Fig. 1b),
 461 the numerical treatment of it is basically averaged. Another
 462 note is that even though fluorescence decay shows different
 463 spectral species, these spectral forms of Chl *a* are not clearly
 464 manifested in the absorption spectrum in both samples.

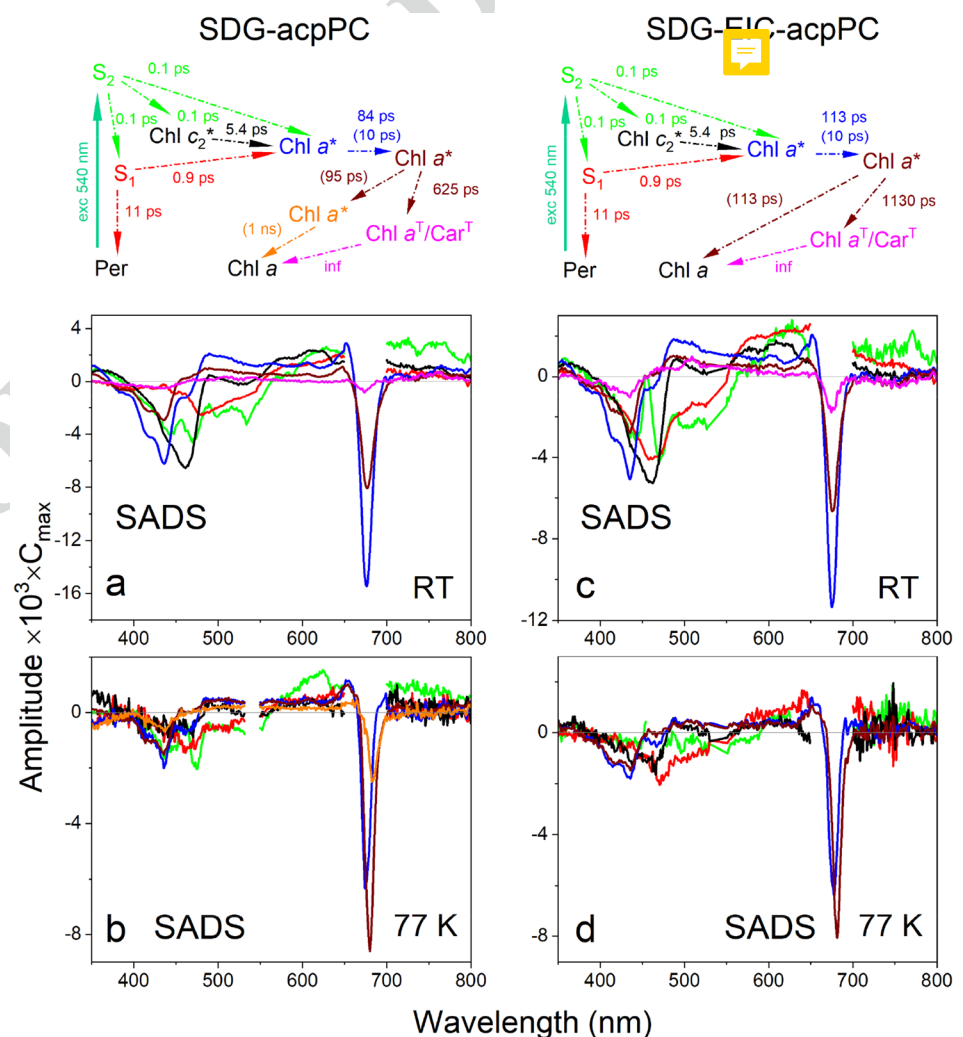
Transient absorption

465
 466 Time-resolved fluorescence imaging data provide useful
 467 information of Chl *a* fluorescence dynamics. This method,
 468 however, does not resolve early events after excitation due
 469 to its low temporal resolution. Since TRF measurement only
 470 monitors light emission, it cannot characterize possible non-
 471 emitting states, which may concurrently form during the
 472 excitation migration within the acpPC oligomeric assembly.
 473 To address this issue, both SDG- and SDG-IEC-acpPC were
 474 subjected to further study of femtosecond time-resolved
 475 transient absorption spectroscopy. The data were collected
 476 at both room temperature (RT) and 77 K, upon excitation
 477 at 540 nm (comparable to TRF). Considering the spectral
 478 reconstruction of the absorption spectrum of SDG-acpPC
 479 shown in Fig. 3a, that wavelength should essentially exclu-
 480 sively excite peridinin and the spectral evolution observed
 481 in the TA profile is associated with excitation energy migra-
 482 tion from peridinin excited states (S_2 and S_1) to Chls. The
 483 data modeling is shown in Fig. 5 (for exemplary raw TA
 484 spectra refer to Fig. S3), and assumes that peridinin (Per)
 485 is excited to S_2 state. The intrinsic lifetime of carotenoid
 486 S_2 state ranges between 100 and 300 fs (Polivka and Sund-
 487 strom 2004). For simplicity, we used the low-end value for
 488 peridinin. If the carotenoid is not energetically coupled to

489 its neighboring Chl *a* or Chl *c* molecules, the excited S_2
 490 state will internally convert to S_1 state that subsequently
 491 will intrinsically decay to the ground state with a lifetime of
 492 11 ps (peridinin, average S_1 state lifetime in polar solvent)
 493 (Bautista et al. 1999; Zigmantas et al. 2001; Zigmantas et al.
 494 2003). Again, for simplicity, it was assumed that peridinin S_1
 495 and S_2 states lifetimes are also temperature independent. TA
 496 data modeling assumes that the S_2 state will be efficiently
 497 transferring excitation to both types of Chls. However, the
 498 carotenoid S_1 state is more fit to transfer excitation energy
 499 to Chl *a* due to a better overlap of peridinin fluorescence
 500 emission and Q_y absorption band of Chl *a*. Because we can-
 501 not temporally resolve excitation transfer from peridinin S_2
 502 state to both Chl *c* and *a*, we assumed that the time constants
 503 are 100 fs, comparable to the state lifetime. The time con-
 504 stant for the S_1 state-related excitation migration route was
 505 then estimated at 0.9 ps. Modeling demonstrated that Chl
 506 c_2 efficiently transfer excitation to Chl *a* with a time con-
 507 stant of 5.4 ps. As if in this case, a customized fitting model
 508 is applied to TA datasets, the fitting results are commonly

509 called species associated difference spectra (SADS) (van
 510 Stokkum et al. 2004). If a model sufficiently mimics the
 511 realistic pathways of the excitation migration/decay, SADS
 512 should very closely correspond to the spectral features
 513 (ground state absorption bleaching (GSB) with accompanied
 514 excited state absorption band (ESA) of individual pigments.
 515 Closer inspection of SADS shows that the profiles fulfill
 516 the criteria particularly for RT TA data. The green SADS,
 517 associated with the S_2 state of peridinin, clearly consists
 518 of bleaching of the ground state absorption accompanied
 519 with a positive band which, based on the previous stud-
 520 ies of a few variants of acpPC complex or peridinin-only
 521 PCP, corresponds to peridinin $S_2 \rightarrow S_n$ ESA band. The red
 522 SADS corresponds to the S_1 state of peridinin and consists
 523 of bleaching of steady-state absorption and adjacent $S_2 \rightarrow S_n$
 524 ESA (Ilagan et al. 2006, Polivka et al. 2006, Schulte et al.
 525 2009a, b, van Stokkum et al. 2009, Niedzwiedzki et al.
 526 2013, Slouf et al. 2013, Niedzwiedzki et al. 2014). The
 527 black SADS is associated with Chl c_2 . The negative part
 528 very adequately corresponds to the bleaching of the Soret

Fig. 5 Global analysis of TA datasets of **a, b** SDG-acpPC and **c, d** SDG-IEC-acpPC preparations performed according to anticipated models of excitation migration pathways presented in the above graphs. It was assumed that excitation at 540 nm will initially promote peridinin (Per) S_2 excited singlet state. Subsequently, excitation energy quickly funnels to Chls *a* directly or via Chl c_2 . Modeling demonstrated that the last stage of the excitation migration pathway alternates at cryogenic temperature. Refer to the main text for more details. Time constants in parentheses (and associated routes) are for 77 K. SADS—species associated decay spectrum, Car—carotenoid (peridinin and/or diadinoxanthin), *—excited states



band and is accompanied by the broad positive ESA, which surpasses the expected bleaching of the Q_y band at ~ 650 nm (Niedzwiadzki et al. 2014). The blue SADS is associated with a pool of excited Chls a populated via excitation energy transfer from peridinin and Chl c_2 . This SADS, associated with excited Chls a , quickly evolves with a time constant of 84–113 ps to another Chl a -related component (brown SADS). At RT, these two SADS are essentially identical in shapes, but the latter has a substantially smaller contribution in the TA datasets (SADS were corrected for their maximal time dependent concentration). Instead of associated with the energetic equilibration of the excited pigment (otherwise, SADS amplitudes should not change but rather shift in position), the 84–113 ps time constant is associated with the depletion of the TA signal, most likely due to singlet–singlet annihilation.

A final pool of the excited Chls (brown SADS) decays with an observed lifetime of 625–1130 ps. These time constants are substantially shorter than the Chl a fluorescence lifetime recorded for the trimeric acpPC (Chl a monomers), which strongly supports the idea of an oligomerization-driven singlet–singlet annihilation. The elongated Chl a fluorescence dynamics in SDG-IEC-acpPC in regard to SDG-acpPC and the same elongated time constants in SDG-IEC-acpPC indicates that additional sample processing progressively disrupts the native oligomerization state of the complex and consequently reduces the probability of the annihilation process occurring between the excited Chls, which are most likely located somewhere at stitching interfaces between each individual trimers in the oligomer. Efficient singlet–singlet annihilation of the excited Chl a observed even at low excitation intensities (shortening of the Chl a fluorescence lifetime) can maximally reduce the chance of formation of Chl a triplets and subsequent sensitization of carotenoid (peridinin/diadinoxanthin) triplets. This is clearly demonstrated for the SDG-acpPC sample, where the combined signals with Chl a and carotenoid triplets were barely seen (magenta SADS). However, once the aggregation level of acpPC changes and the lifetime of the longer-lived Chl a subsequently elongates, the population of Chl a /carotenoid triplets grows (compare magenta SADS in Fig. 5a and c). Notable difference induced at 77 K is that the acpPC oligomers do not reveal any detectable accumulation of Chl a /peridinin triplets (no magenta SADS). The dynamics of the excited singlet state of Chl a is also altered. Overall, it is substantially faster and reduces formation of Chl a triplets.

At this point, the TRF and TA analysis have given some complementary characteristics of the excited Chls a at 77 K. In summary, for the SDG-acpPC sample, both TA and TRF fitting data have revealed that there are three spectro-kinetic components associated with Chl a . Considering that the TA lifetime results support that the excited Chls may be additionally affected by excitation annihilation, the following

conclusions can be reached. The F682 SAFS component parallels the blue SADS with the observed bleaching of the Q_y band at 676 nm. The F687 SAFS corresponds to the brown SADS with the observed bleaching of the Q_y band at 681 nm, and the F695 SAFS would correspond to the orange SADS with the observed bleaching of the Q_y band at 684 nm. Note that it is still misleading to directly match the SAFS to the SADS components in terms of the positions of their fluorescence maxima and bleaching minima (e.g., F682 SAFS and 681 nm SADS) a . In the TA spectrum, the observed “bleaching” of the Chl a Q_y band corresponds to a collective signals of the real bleaching of the Q_y absorption band and the probe-driven stimulated emission (fluorescence emission). Since the detector unfortunately doesn't have the resolution of discriminating between them (due to the nature of the instrumental setting), the recorded “bleaching” band simply represents a combination of both, and a collective peak is detected, with a minima located around halfway between the maxima of the absorption band and the fluorescence emission.

Discussion

Our purification and biochemical characterizations of the acpPC complexes from dinoflagellate *Fugacium kawagutii* in this study illustrates that higher order structure organizations of the acpPC antenna complex can be kept intact and isolated if appropriate buffers and purification protocols are followed. All these rely on the use of high molarity of betaine in the preparation buffers, which has been successfully used for reaction centers isolation in multiple organisms. It should be noted that the higher order oligomeric structure of acpPC can be disrupted and reassembled *in vitro* experiments, resulting in a heterogenous mixture (SDG-IEC) (Fig. 1b, right panel). Spectroscopically, they are not exactly the same as the original nonameric form (SDG). It seems that the single-step sucrose density gradient ultracentrifugation (without extensive chromatography) represents a much milder isolation strategy that keeps the protein complex in its native-like state and relatively high purity (Fig. 1c). The pigment composition analysis of SDG-acpPC of SDG-IEC-acpPC indicates that further biochemical processing (adsorption to the chromatography resin and washing in the presence of detergents that have to be included in the reagent buffers) tends to reduce the pigment content. At present time, there are no 3-D structural studies from either protein X-ray crystallography or cryo-EM, we do not know where and how the (stripped) pigments may have interacted with the apo-protein in nonameric acpPC or with the other cofactors in the complex. Hydrophobic interactions in LHC are usually the major force stabilizing the pigments and their associated binding partners, such as membrane lipids. The

632 more native lipids the protein samples retain, the more pig- 685
 633 ments are found stabilized in the biochemical preparations 686
 634 (Buchel 2003; Beer et al. 2006; Lepetit et al. 2010). Appar- 687
 635 ently, extensive exposure of the solubilized samples to the 688
 636 detergents which are necessarily used in the biochemical 689
 637 buffers during IEC will inevitably strip off those loosely 690
 638 bound pigments. Those pigments may be located either on 691
 639 the surface of the acpPC nonamer or the interfaces between 692
 640 each subunit in the oligomer. Previously, it has been reported 693
 641 that in the FMO antenna complex containing bacteriochloro- 694
 642 phyll *a* (BChl *a*), the eighth BChl *a* pigment, located in the 695
 643 interface of trimeric FMO, can be easily lost during purifica- 696
 644 tion owing to surface exposure (Wen et al. 2011) and (Wen 697
 645 et al. 2011). Here, we could reasonably suspect a similar 698
 646 situation could occur for the nonameric acpPC. Please note, 699
 647 the eighth pigment discovery in FMO has a huge impact on 700
 648 the excitation energy research in the research community. 701
 649 We highly recommend our SDG method for future acpPC 702
 650 and its relevant research. Based on findings presented in this 703
 651 study, the overall picture is that the native acpPC is pre- 704
 652 dominantly clustered to larger acpPC oligomers, most likely 705
 653 trimer of trimers (nonamer), acpPC^(3 × 3). 706

654 Previous time-resolved fluorescence analysis on oligom- 707
 655 ers of the major LHC in higher plants indicated that the 708
 656 oligomerized LHC trimers tend to form a weakly coupled 709
 657 inter-trimer Chl *a*-Chl *a* excitation state. They are charac- 710
 658 terized by a strongly far-red enhanced fluorescence spectrum, 711
 659 strikingly similar to the fluorescence component observed in 712
 660 intact leaves when NPQ is induced (Miloslavina et al. 2008). 713
 661 Our time-resolved spectroscopic studies on the oligomeric 714
 662 acpPC in this research show similar Chl *a* fluorescence 715
 663 characteristics as observed in higher plants. A very inter- 716
 664 esting question that immediately arises is how this acpPC 717
 665 oligomer interacts with RCs, such as photosystem II (PSII). 718
 666 Unfortunately, the modified purification protocol is still 719
 667 not adequate for successful separation of PSII, most likely 720
 668 because the photosystems are extremely fragile and fall apart 721
 669 during ever-known gentle detergent treatment of the thy- 722
 670 lakoid membrane. Another interesting aspect is how such 723
 671 oligomeric representation of acpPC (nonamer) is natively 724
 672 preferred. Uncoincidentally, recent structural determinations 725
 673 on more intact algal PSII-LHCII supercomplex showed that 726
 674 the major LHC complex forms closely associated trimer of 727
 675 LHCII trimers, i.e., nonamer, which is then coupled to the 728
 676 photosystem core complex via minor light-harvesting CP29 729
 677 complex (Burton-Smith et al. 2019; Shen et al. 2019).

678 Spectroscopically, the nonameric acpPC is substantially 729
 679 different than its trimeric counterpart. The differences are 730
 680 readily seen in steady-state absorption and fluorescence 731
 681 emission spectra at 77 K. The most interesting findings, 732
 682 however, come from the completely different dynamics of 733
 683 the excited states of the acpPC-bound Chls *a* among the oli-
 684 gomeric and trimeric acpPC. Previous work showed that in

685 acpPC trimer, the excited Chl *a* is uniform and has one spec- 686
 687 tral form with a mono-exponential component decay with 688
 689 a lifetime of ~5.8 ns (at 77 K) (Niedzwiedzki et al. 2014). 690
 691 Those studies showed that the acpPC trimer is spectroscopi- 692
 693 cally very homogenous without any spectral heterogeneity 694
 695 that could benefit the excitation migration downhill to a spe- 696
 697 cific site in the trimer assembly. This picture is completely 698
 699 altered in the more native oligomeric assembly studied in 700
 701 this work. The fluorescence components with red-shifted 702
 703 emission peaks may represent a characteristic marker for 704
 705 NPQ condition in *Symbiodiniaceae* cells under photopro- 706
 707 tection model. The time-resolved fluorescence and transient 708
 709 absorption studies also demonstrated the presence of three 709
 710 spectrally and dynamically different forms of excited Chl 710
 711 *a*. Excitation dynamics of these pigments show that excita- 711
 712 tion very likely spatially migrates within the oligomer to a 712
 713 specific site due to unidirectional energetic funneling from 713
 714 the energetically highest to lowest Chls. Hypothetically, it 714
 715 is possible that this mechanism somehow maneuvers exci- 715
 716 tations from photons absorbed in random places within the 716
 717 oligomeric assembly into a specific location that could ulti- 717
 718 mately transfer it to the adjacent PSII access point or to a 718
 719 non-photochemical quenching center if hopping of excita- 719
 720 tion to PSII is not possible (or a closed PSII). Research on 720
 721 the NPQ candidate proteins in this species is underway. 721

712 **Supplementary Information** The online version contains supplemen- 712
 713 tary material available at <https://doi.org/10.1007/s11120-022-00951-6>. 713

714 **Acknowledgements** The authors thank Atsuko Kanazawa in David 714
 715 Kramer's lab for sharing the *Fugacium kawagutii* strain and helpful 715
 716 discussion. D.N.M. acknowledges Center for Solar Energy and Energy 716
 717 Storage at McKelvey School of Engineering at Washington University 717
 718 in Saint Louis for financial support. N.C. M. M. was supported by the 718
 719 U.S. Department of Energy (DOE), Office of Basic Energy Sciences 719
 720 under grant DE-CD0002036 to Professors: Chris Kirmaier and Dewey 720
 721 Holten. This research was supported by the Danforth Seed Grant of 721
 722 Department of Biology at Washington University in Saint Louis (to 722
 723 H.L.). H. L. also acknowledges the U.S. Department of Energy (DOE), 723
 724 Office of Basic Energy Sciences, Photosynthetic Systems (PS) Program 724
 725 (Grant DE-FG02-07ER15902 to H.L.). 725

726 **Funding** This study was supported by U.S. Department of Energy 726
 727 (Grant No. DE-FG02-07ER15902, DE-CD0002036), and Danforth 727
 728 Foundation, Seed grant Biology Washington University. 728

729 Declarations

730 **Conflict of interest** The authors have no competing interests to declare 730
 731 that are relevant to the content of this article. 731

732 References

733 Bautista JA, Connors RE, Raju BB, Hiller RG, Sharples FP, Gosztola 733
 734 D, Wasielewski MR, Frank HA (1999) Excited state properties 734
 735 of peridinin: observation of a solvent dependence of the lowest 735

- 734 excited singlet state lifetime and spectral behavior unique among
735 carotenoids. *J Phys Chem B* 103(41):8751–8758
- 736 Beer A, Gundermann K, Beckmann J, Buchel C (2006) Subunit com-
737 position and pigmentation of fucoxanthin-chlorophyll proteins in
738 diatoms: evidence for a subunit involved in diadinoxanthin and
739 diatoxanthin binding. *Biochemistry* 45(43):13046–13053
- 740 Blankenship RE (2002) "Antenna complexes and energy transfer pro-
741 cesses." *Mol Mech Photosynth* 61–94.
- 742 Buchel C (2003) Fucoxanthin-chlorophyll proteins in diatoms: 18 and
743 19 kDa subunits assemble into different oligomeric states. *Bio-
744 chemistry* 42(44):13027–13034
- 745 Buchel C (2015) Evolution and function of light harvesting proteins. *J
746 Plant Physiol* 172:62–75
- 747 Burton-Smith RN, Watanabe A, Tokutse R, Song CH, Murata K,
748 Minagawa J (2019) Structural determination of the large pho-
749 tosystem II?light-harvesting complex II supercomplex of *Chla-
750 mydomonas reinhardtii* using nonionic amphipol. *J Biol Chem*
751 294(41):15003–15013
- 752 Di Valentin M, Salvadori E, Agostini G, Biasibetti F, Ceola S, Hiller R,
753 Giacometti GM, Carbonera D (2010) Triplet-triplet energy trans-
754 fer in the major intrinsic light-harvesting complex of *Amphidinium
755 carterae* as revealed by ODMR and EPR spectroscopies. *BBA-
756 Bioenergetics* 1797(10):1759–1767
- 757 Durnford DG, Deane JA, Tan S, McFadden GI, Gantt E, Green BR
758 (1999) A phylogenetic assessment of the eukaryotic light-har-
759 vesting antenna proteins, with implications for plastid evolution.
760 *J Mol Evol* 48(1):59–68
- 761 Hiller RG, Wrench PM, Gooley AP, Shoebridge G, Breton J (1993)
762 The major intrinsic light-harvesting protein of *Amphidinium* -
763 characterization and relation to other light-harvesting proteins.
764 *Photochem Photobiol* 57(1):125–131
- 765 Hiller RG, Wrench PM, Sharples FP (1995) The light-harvesting chlo-
766 rophyll *a-c*-binding protein of dinoflagellates—a putative polypro-
767 tein. *FEBS Lett* 363(1–2):175–178
- 768 Hofmann E, Wrench PM, Sharples FP, Hiller RG, Welte W, Dieder-
769 icks K (1996) Structural basis of light harvesting by carotenoids:
770 peridinin-chlorophyll-protein from *Amphidinium carterae*. *Science*
771 272(5269):1788–1791
- 772 Iglesiasprieto R, Govind NS, Trench RK (1991) Apoprotein composi-
773 tion and spectroscopic characterization of the water-soluble peri-
774 dinin chlorophyll alpha-proteins from 3 symbiotic dinoflagellates.
775 *Proc R Soc B-Biol Sci* 246(1317):275–283
- 776 Ilagan RP, Kosciielecki JF, Hiller RG, Sharples FP, Gibson GN, Birge
777 RR, Frank HA (2006) Femtosecond time-resolved absorption
778 spectroscopy of main-form and high-salt peridinin-chlorophyll
779 *a*-proteins at low temperatures. *Biochemistry* 45:14052–14063
- 780 Jiang J, Zhang H, Orf GS, Lu Y, Xu W, Harrington LB, Liu H, Lo CS,
781 Blankenship RE (2014) Evidence of functional trimeric chloro-
782 phyll *a/c2*-peridinin proteins in the dinoflagellate *Symbiodinium*.
783 *Biochim Biophys Acta* 1837(11):1904–1912
- 784 Kanazawa A, Blanchard GJ, Szabo M, Ralph PJ, Kramer DM (2014)
785 The site of regulation of light capture in *Symbiodinium*: does the
786 peridinin-chlorophyll *a*-protein detach to regulate light capture?
787 *Biochim Biophys Acta* 1837(8):1227–1234
- 788 Lepetit B, Volke D, Gilbert M, Wilhelm C, Goss R (2010) Evidence for
789 the existence of one antenna-associated, lipid-dissolved and two
790 protein-bound pools of diadinoxanthin cycle pigments in diatoms.
791 *Plant Physiol* 154(4):1905–1920
- 792 Liu ZF, Yan HC, Wang KB, Kuang TY, Zhang JP, Gui LL, An
793 XM, Chang WR (2004) Crystal structure of spinach major
794 light-harvesting complex at 2.72 angstrom resolution. *Nature*
795 428(6980):287–292
- 796 Miloslavina Y, Wehner A, Lambrev PH, Wientjes E, Reus M, Garab
797 G, Croce R, Holzwarth AR (2008) Far-red fluorescence: a direct
798 spectroscopic marker for LHCII oligomer formation in non-pho-
799 tochemical quenching. *FEBS Lett* 582(25–26):3625–3631
- Niedzwiedzki DM, Fuciman M, Frank HA, Blankenship RE (2011) 800
Energy transfer in an LH4-like light harvesting complex from the 801
aerobic purple photosynthetic bacterium *Roseobacter denitrifi-* 802
cans. *Biochem Biophys Acta* 1807(5):518–528 803
- Niedzwiedzki DM, Jiang J, Lo CS, Blankenship RE (2013) Low-tem- 804
perature spectroscopic properties of the peridinin-chlorophyll 805
a-protein (PCP) complex from the coral symbiotic dinoflagellate 806
Symbiodinium. *J Phys Chem B* 117(38):11091–11099 807
- Niedzwiedzki DM, Jiang J, Lo CS, Blankenship RE (2014) Spectro- 808
scopic properties of the chlorophyll *a*-chlorophyll *c* (2)-peridinin- 809
protein-complex (acpPC) from the coral symbiotic dinoflagellate 810
Symbiodinium. *Photosynth Res* 120(1–2):125–139 811
- Polivka T, Sundstrom V (2004) Ultrafast dynamics of carotenoid 812
excited states—from solution to natural and artificial systems. 813
Chem Rev 104(4):2021–2071 814
- Polivka T, van Stokkum IH, Zigmantas D, van Grondelle R, Sundstrom 815
V, Hiller RG (2006) Energy transfer in the major intrinsic light- 816
harvesting complex from *Amphidinium carterae*. *Biochemistry* 817
45(28):8516–8526 818
- Reynolds JM, Bruns BU, Fitt WK, Schmidt GW (2008) Enhanced 819
photoprotection pathways in symbiotic dinoflagellates of shal- 820
low-water corals and other cnidarians. *Proc Natl Acad Sci U S A* 821
105(36):13674–13678 822
- Schagger H, von Jagow G (1991) Blue native electrophoresis for isola- 823
tion of membrane protein complexes in enzymatically active form. 824
Anal Biochem 199(2):223–231 825
- Schulte T, Niedzwiedzki DM, Birge RR, Hiller RG, Polivka T, Hof- 826
mann E, Frank HA (2009a) Identification of a single peridinin 827
sensing Chl-*a* excitation in reconstituted PCP by crystallography 828
and spectroscopy. *Proc Natl Acad Sci USA* 106(49):20764–20769 829
- Schulte T, Sharples FP, Hiller RG, Hofmann E (2009b) X-ray struc- 830
ture of the high-salt form of the peridinin-chlorophyll *a*-protein 831
from the dinoflagellate *Amphidinium carterae*: Modulation of the 832
spectral properties of pigments by the protein environment. *Bio-
833 chemistry* 48(21):4466–4475 834
- Schulte T, Johanning S, Hofmann E (2010) Structure and function of 835
native and refolded peridinin-chlorophyll-proteins from dinoflag- 836
ellates. *Eur J Cell Biol* 89(12):990–997 837
- Sharples FP, Wrench PM, Ou KL, Hiller RG (1996) Two distinct forms 838
of the peridinin-chlorophyll alpha-protein from *Amphidinium* 839
carterae. *BBA-Bioenergetics* 1276(2):117–123 840
- Shen LL, Huang ZH, Chang SH, Wang WD, Wang JF, Kuang TY, Han 841
GY, Shen JR, Zhang X (2019) Structure of a C2S2M2N2 type 842
PSII-LHCII supercomplex from the green alga *Chlamydomonas* 843
reinhardtii. *Proc Natl Acad Sci USA* 116(42):21246–21255 844
- Slouf V, Fuciman M, Johanning S, Hofmann E, Frank HA, Polivka T 845
(2013) Low-temperature time-resolved spectroscopic study of the 846
major light-harvesting complex of *Amphidinium carterae*. *Photo-
847 synth Res* 117(1–3):257–265 848
- van Stokkum IH, Larsen DS, van Grondelle R (2004) Global and 849
target analysis of time-resolved spectra. *Biochim Biophys Acta* 850
1657(2–3):82–104 851
- van Stokkum IH, Papagiannakis E, Vengris M, Salverda JM, Polivka 852
T, Zigmantas D, Larsen DS, Lampoura SS, Hiller RG, van Gron- 853
delle R (2009) Inter-pigment interactions in the peridinin chloro- 854
phyll protein studied by global and target analysis of time resolved 855
absorption spectra. *Chem Phys* 357(1–3):70–78 856
- Vinklarek IS, Bornemann TLV, Lokstein H, Hofmann E, Alster J, 857
Psencik J (2018) Temperature dependence of chlorophyll tri- 858
plet quenching in two photosynthetic light-harvesting com- 859
plexes from higher plants and dinoflagellates. *J Phys Chem B* 860
122(38):8834–8845 861
- Wang WD, Yu LJ, Xu CZ, Tomizaki T, Zhao SH, Umena Y, Chen XB, 862
Qin XC, Xin YY, Suga M, Han GY, Kuang TY, Shen JR (2019) 863
Structural basis for blue-green light harvesting and energy dis- 864
sipation in diatoms. *Science* 363(6427):598 865

- 866 Wen J, Zhang H, Gross ML, Blankenship RE (2011) Native electro- 879
 867 spray mass spectrometry reveals the nature and stoichiometry of 880
 868 pigments in the FMO photosynthetic antenna protein. *Biochem-*
 869 *istry* 50(17):3502–3511
- 870 Zigmantas D, Polivka T, Hiller RG, Yartsev A, Sundstrom V (2001) 881
 871 Spectroscopic and dynamic properties of the peridinin lowest sin- 882
 872 glet excited states. *J Phys Chem A* 105(45):10296–10306
- 873 Zigmantas D, Hiller RG, Sundstrom V, Polivka T (2002) Carotenoid to 883
 874 chlorophyll energy transfer in the peridinin-chlorophyll-*a*-protein 884
 875 complex involves an intramolecular charge transfer state. *Proc* 885
 876 *Natl Acad Sci USA* 99(26):16760–16765
- 877 Zigmantas D, Hiller RG, Yartsev A, Sundstrom V, Polivka T (2003) 886
 878 Dynamics of excited states of the carotenoid peridinin in polar 887
 solvents: dependence on excitation wavelength, viscosity, and
 temperature. *J Phys Chem B* 107(22):5339–5348
- Publisher's Note** Springer Nature remains neutral with regard to 881
 jurisdictional claims in published maps and institutional affiliations. 882
- Springer Nature or its licensor holds exclusive rights to this article under 883
 a publishing agreement with the author(s) or other rightsholder(s); 884
 author self-archiving of the accepted manuscript version of this article 885
 is solely governed by the terms of such publishing agreement and 886
 applicable law. 887

UNCORRECTED PROOF

Journal:	11120
Article:	951

Author Query Form

Please ensure you fill out your response to the queries raised below and return this form along with your corrections

Dear Author

During the process of typesetting your article, the following queries have arisen. Please check your typeset proof carefully against the queries listed below and mark the necessary changes either directly on the proof/online grid or in the 'Author's response' area provided below

Query	Details Required	Author's Response
AQ1	Please confirm the section headings are correctly identified.	
AQ2	Kindly check and confirm the processed affiliation is correctly identified.	
AQ3	Please provide the complete details for the reference Blankenship, (2002).	
AQ4	Please confirm if the author names are presented accurately and in the correct sequence. Given name: [Nikki] [Cecil] [M.] Last name [Magdaong]. Also, kindly confirm the details in the metadata are correct.	